Pharm Res (2013) 30:238–246
DOI 10.1007/s11095-012-0868-4

RESEARCH PAPER

Electrospun Formulations Containing Crystalline Active Pharmaceutical Ingredients

Blair Kathryn Brettmann • Kamyu Cheng • Allan S. Myerson • Bernhardt L. Trout

Received: 3 May 2012 / Accepted: 15 August 2012 / Published online: 25 August 2012

ABSTRACT

Purpose To investigate the use of electrospinning for forming solid dispersions containing crystalline active pharmaceutical ingredients (API) and understand the relevant properties of the resulting materials.

Method Free surface electrospinning was used to prepare nanofiber mats of poly(vinyl pyrrolidone) (PVP) and crystalline albendazole (ABZ) or famotidine (FAM) from a suspension of the drug crystals in a polymer solution. SEM and DSC were used to characterize the dispersion, XRD was used to determine the crystalline polymorph, and dissolution studies were performed to determine the influence of the preparation method on the dissolution rate.

Results The electrospun fibers contained 31 wt% ABZ and 26 wt% FAM for the 1:2 ABZ:PVP and 1:2 FAM:PVP formulations, respectively, and both APIs retained their crystalline polymorphs throughout processing. The crystals had an average size of about 10 μm and were well-dispersed throughout the fibers, resulting in a higher dissolution rate for electrospun tablets than for powder tablets.

Conclusions Previously used to produce amorphous formulations, electrospinning has now been demonstrated to be a viable option for producing fibers containing crystalline API. Due to the dispersion of the crystals in the polymer, tablets made from the fiber mats may also exhibit improved dissolution properties over traditional powder compression.

KEY WORDS crystals · electrospinning · formulation · solid dispersion

B. K. Brettmann · K. Cheng · A. S. Myerson · B. L. Trout (✉)
Department of Chemical Engineering
Massachusetts Institute of Technology
50 Ames St., E19-502b
Cambridge, Massachusetts 02139, USA
e-mail: trout@mit.edu

ABBREVIATIONS

ABZ	albendazole
API	active pharmaceutical ingredient
DSC	differential scanning calorimetry
FAM	famotidine
PVP	poly(vinyl pyrrolidone)
SEM	scanning electron microscopy
XRD	X-ray diffraction
A	surface area for diffusion
C	concentration in solution
C_{sat}	solubility
D	diffusion coefficient
$\frac{dm}{dt}$	dissolution rate
g	gravitational acceleration
h	diffusional path length
ρ_f	density of the fluid
ρ_p	density of the particle
R	radius of the particle
μ	viscosity of the fluid
v_s	settling velocity

INTRODUCTION

Although several industries, including chemical, food, and petrochemical, have made the transition from batch to continuous manufacturing, the pharmaceutical industry has lagged behind. The cost disadvantages of a batch process have not been sufficiently high to overcome the regulatory and control challenges or the cost of developing new continuous manufacturing technology for the production of pharmaceutical products. Lately, however, a changing regulatory atmosphere as well as an increasingly difficult and competitive market are driving investment into the development of continuous manufacturing operations (1).

Downstream pharmaceutical processing is one area with a particular need for improvement. Going from purified active pharmaceutical ingredient (API) to a final, formulated product typically involves many costly drying, granulation, blending and milling steps. Various continuous processes have been proposed to decrease the number of powder handling steps and provide efficient blending of API and excipients including melt extrusion (2,3), thin film casting (4) and electrospinning (5–9). Though a less-traditional technique, electrospinning has distinct advantages over extrusion and thin film casting. Because of the high surface area generated during electrospinning, the evaporation rate of the solvent is incredibly high, allowing for more efficient drying at ambient temperatures than is possible with thin film casting. In addition, no heat is necessary to blend ingredients during electrospinning, as they are already well blended in the liquid solution prior to spinning, making it more applicable for heat-sensitive API than melt extrusion.

In electrospinning, fibers of 20–2000 nm diameter are produced from a solution of a polymer, solvent and any desired additives. With a traditional single needle electrospinning process, the solution is charged and pumped through a needle, forming a drop at the tip. When the charge repulsion forces overcome the surface tension forces, the drop deforms into a conical form called the Taylor cone and a jet extends from the tip. The fiber thins and dries as it travels towards a grounded collection plate, resulting in a non-woven mat of dried fibers (10).

This single-needle electrospinning approach, however, has a low production rate, on the order of 1 mg solids/min for the materials used in this study. This is insufficient for application to an industrial manufacturing process, and so we use a newer technology for the scale up of electrospinning, referred to as "free surface electrospinning" or "needleless electrospinning." In free surface electrospinning, jetting occurs from a free liquid surface, such as a film on a rotating drum, disk or wire spindle or from the surface of gaseous bubbles (11–20). This results in the formation of multiple Taylor cones and jets and a high production rate, on the order of 20 mg/min for the materials and equipment used in this study. The free surface electrospinning technique has previously been adapted as a commercial unit and is available through Elmarco (Liberec, Czech Republic).

Though scale-up of electrospinning is possible with approaches such as free surface electrospinning, a further challenge prevents the technique from being applied to pharmaceutical manufacturing. Due to the rapid solvent evaporation during electrospinning, the drug is often present in the resulting fibers in its amorphous form (7–9,21,22). This can be advantageous for poorly water soluble drugs, as the amorphous form often has a higher water solubility than the crystalline form, but it also introduces physical stability issues, with the amorphous API crystalizing over time (23). For this technique to become generally applicable as a manufacturing process, it must also be able to produce fibers containing crystalline API.

A few studies on electrospinning of API have found that the API is in its crystalline form immediately after electrospinning (24–26). All three studies used a polymer that itself crystallizes during electrospinning, either polycaprolactone or poly(ethylene oxide). Natu *et al.* found that the API was partially crystalline in only one formulation examined, that with greater than 10% w/w API (25), and Ignatious *et al.* determined that, at drug loadings higher than 35.9% w/w, nabumetone exhibits a melting endotherm when analyzed immediately after electrospinning (26). These studies have demonstrated that obtaining crystalline API in electrospun fibers is possible by spinning a solution of API and polymer; however, the API is only partially crystalline and the controlling factors are poorly understood.

In this work, we take an alternative approach to producing fibers containing crystalline API and electrospin API crystals suspended in a polymer solution. It has previously been demonstrated that nano- and microparticles can be electrospun starting from a dispersion of the particles in a polymer solution. The particles can be very small, 20 nm or less, as with magnetite (27) and carbon black (28) or larger, 1–10 μm, as with bacteria and viruses (29), clays (30,31) and polystyrene beads (32,33). Though most studies on electrospinning of particles have been done using a single needle apparatus, we recently demonstrated that polystyrene beads of 1–10 μm diameter can be electrospun from PVP solutions using free surface electrospinning (32).

We use free surface electrospinning to spin suspensions of API crystals in a poly(vinyl pyrrolidone) (PVP)/ethanol solution. If a solvent is chosen in which the API is insoluble, the API will maintain its crystallinity during the electrospinning process, resulting in electrospun mats containing crystalline drug dispersed within the polymer fibers. For this work, we selected two poorly water-soluble APIs that are practically insoluble in ethanol (34), albendazole (ABZ) and famotidine (FAM), and chose PVP as the polymer due to its acceptance as a pharmaceutical excipient and the ease of electrospinning. We demonstrate that the API crystals are entrained within the fibers, retain their crystalline morphology during the process, and exhibit improved dissolution rates when compared to compressed powder tablets.

MATERIALS AND METHODS

Materials

PVP (1.3 MDa molecular weight), FAM and ABZ were purchased from Sigma-Aldrich (St. Louis, MO) and

American Chemical Society grade ethanol was purchased from VWR International (West Chester, PA).

Electrospinning

To prepare the 1:2 API:polymer electrospinning solutions, 8.6 wt% PVP was dissolved in ethanol and 4.3 wt% API was added to the solution and suspended by stirring. Immediately prior to electrospinning, the solution was sonicated using a Sonics Vibra-cell serial number 48265 T ultrasonic processor with a tapered microtip (Sonics and Materials, Newtown, CT) in order to ensure that the particles were well-suspended at the start of the electrospinning process. Sonication was performed three times for 40 s each time, with at least 30 s delay between each at 40% maximum amplitude to prevent overheating.

A schematic for the free surface electrospinning apparatus is shown in Fig. 1. A wire spindle rotates through the charged suspension bath containing the API/polymer/solvent mixture. As the spindle crosses the air/fluid interface, a thin layer of fluid is entrained on the wire, which breaks into droplets due to Plateau-Rayleigh instabilities (20). Under a sufficiently high applied electric field, the droplets jet and a fiber extends towards the grounded collection plate (upwards in this configuration). Electrospinning of each droplet continues until the droplet is depleted or the electric field condition is no longer met. A detailed description of the mechanism of free surface electrospinning can be found in Ref. 20.

Key process parameters in free surface electrospinning and their values for these experiments are listed in Table I.

Characterization

Scanning electron microscopy (SEM) was used to analyze the morphology of the fibers. A Quorum Technologies SC7640 high resolution gold/palladium sputter coater was used to coat the samples and a JEOL 6060 SEM at 5 kV operating voltage was used to obtain images.

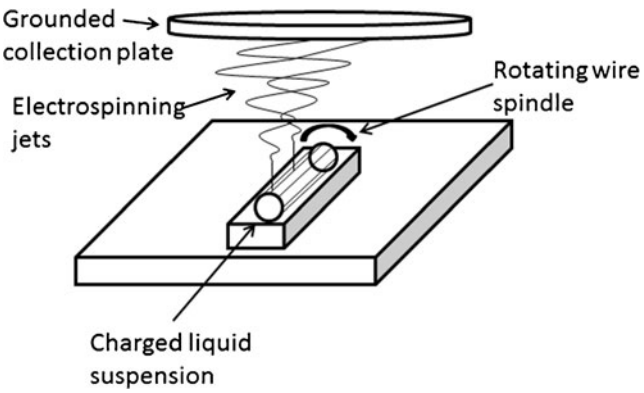

Fig. 1 Schematic of the free surface electrospinning apparatus consisting of a rotating wire spindle, a charged bath for the liquid suspension, and a grounded collection plate.

Both X-ray diffraction (XRD) and differential scanning calorimetry (DSC) were used to confirm the presence of crystals and analyze the polymorph present in the electrospun fibers. XRD was performed on a PANalytical X'Pert Pro with a reflection-transmission spinner PW 3064/60 sample stage and a Cu X-ray source with a 1.54 Å wavelength. DSC was performed on a TA DSC Q2000 instrument using a 2–6 mg sample in an aluminum sample pan. The materials were heated at 10°C/min to 250°C and 200°C for ABZ and FAM, respectively.

Particle size analysis was performed on the spinning solutions prior to sonication, after sonication, and 1 h after sonication. A Malvern Mastersizer 2000 with a Hydro 2000μP accessory was used to measure the particle size distribution and the volume-based results were used for the analysis. Three measurements were made per sample and the average is reported in this work.

In order to determine the actual drug loading in the electrospun fibers, samples were analyzed with a Perkin-Elmer (Waltham, MA) double-beam Lambda25 UV-vis spectrophotometer. A standard curve was prepared for ABZ in methanol for concentrations from 0.005 mg/mL to 0.05 mg/mL at an absorbance of 295 nm and for FAM in methanol for concentrations from 0.002 mg/mL to 0.035 mg/mL at an absorbance of 286 nm. PVP does not absorb in the UV range and pure methanol was used for the background spectrum. A known mass of electrospun mat was dissolved in a known volume of methanol and diluted such that the expected concentration of API fell within the concentration ranges covered by the standard curves. From the resulting measured concentration, the mass of API in the original mat sample, and thus the weight percent API in the electrospun mat was calculated. Three measurements were made per API and were averaged to give the reported value.

Dissolution

Tablets were made from electrospun material by weighing out 150 mg material and pressing into a 9 mm tablet using a

Table I Parameters Used in Electrospinning Experiments

Parameter	Value
Distance from apex of spindle to grounded plate	20 cm
Applied voltage	30–35 kV
Rotation rate	8.8 rpm
Spindle type	Wire electrode, 5 wires

Gamlen Tablet Press model GTP1. Powder tablets were prepared by weighing out 50 mg API powder and 100 mg PVP powder, mixing for 1 min, and pressing into 9 mm tablets using the same press with the same insertion depth. The electrospun tablets were compared to the compressed powder tablets for analysis. Market formulations of APIs were not used for comparison because we aim to examine only the effects of using the electrospinning preparation method compared to a powder-based preparation method. Electroprocessed materials may be further optimized for better dissolution through the use of additional excipients in the same manner as is done for a market formulation and then the two may be compared.

Dissolution was performed using a Varian VK 7025 dissolution bath (Agilent, Santa Clara, CA) and a Cary 50 Bio UV spectrophotometer (Agilent, Santa Clara, CA). For ABZ we used the standard USP method with 900 mL 0.1 N HCl media, apparatus II, 50 rpm paddle speed and a temperature of 37°C. For FAM we used the standard USP method with 900 mL 0.1 M Phosphate buffer media, apparatus II, 50 rpm paddle speed, and a temperature of 37°C. Measurements were made every minute for 90 min by probes inserted in the bath and connected to the spectrophotometer by fiber optic cables.

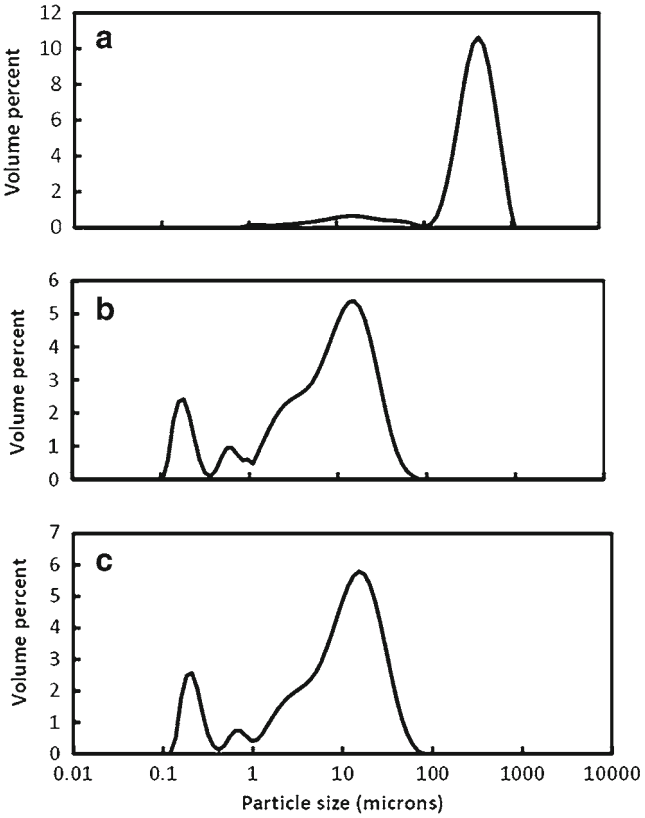

Fig. 2 Particle size distribution of 4.3 wt% ABZ crystals suspended in 8.6 wt% PVP in ethanol (**a**) before sonication, (**b**) after sonication, (**c**) after 1 h.

RESULTS

Particle Size Analysis

The particle size distributions of the API crystals suspended in the PVP/ethanol solution were measured prior to sonication, after sonication and after standing for 1 h, approximately the length of time to electrospin the mat for analysis. The distributions for the ABZ and FAM suspensions are shown in Figs. 2 and 3.

For ABZ, the sonication greatly decreases the crystal size. This is likely due to dispersal of aggregates rather than crystal breakage, as SEM images of the ABZ crystals show agglomerates of smaller crystals (Fig. 4a). The FAM particle size distribution does not show a strong change following sonication. This is likely because the FAM crystals are not present as agglomerates in the powder, as can be seen in Fig. 4b. Following 1 h of standing, both suspensions retain their particle size distribution, indicating that the suspensions electrospun will retain their particle size distribution throughout the 1 h electrospinning process used in this work.

SEM

The morphology of the electrospun fibers were examined by SEM and the images are shown in Fig. 5. In both cases, the API crystals present in the electrospun fibers are easily visible. For the ABZ dispersed in the PVP mat, the crystals are present in the fibers as small agglomerates as well as dispersed crystals, which can be seen by careful examination of the roughness of the fibers, particularly in Fig. 5c. FAM dispersed within PVP, on the other hand, shows little agglomeration. It is interesting to note that the FAM crystals are always distributed with their longest side parallel to the fiber. This can be attributed to the high shear forces during jetting (35).

Crystallinity

XRD and DSC were both used to examine the crystallinity of the API within the electrospun fibers. For 1:2 ABZ:PVP, the melting endotherm is broad with an onset melting point of 165°C, indicating that the ABZ is crystalline in the fibers (Fig. 6). The onset melting point is depressed from that of the crystalline ABZ as received, 190°C. The onset melting of ABZ is consistent with that of Form I of ABZ shown in the literature (36).

The first onset melting point for crystalline FAM as received is 160°C, and based on the DSC results (Fig. 7), there is a broad melting endotherm for the 1:2 FAM:PVP with an onset at 150°C. This melting point corresponds to polymorph B (37). There is a second melting endotherm for the crystalline

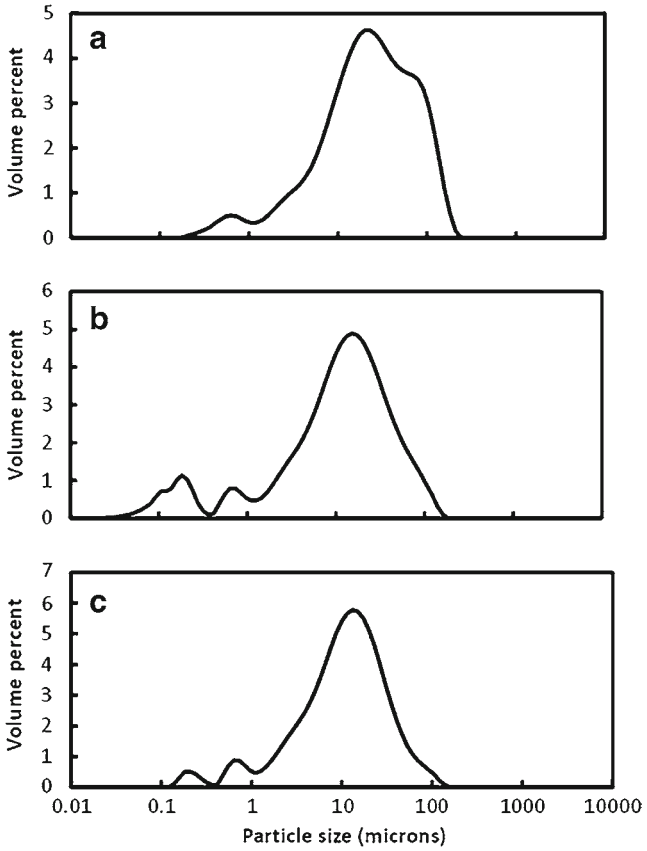

Fig. 3 Particle size distribution of 4.3 wt% FAM crystals suspended in 8.6 wt% PVP in ethanol (**a**) before sonication, (**b**) after sonication, (**c**) after 1 h.

material as received with on onset at 167°C corresponding to polymorph A (37). This melting endotherm is also present for the 1:2 FAM:PVP electrospun material with an onset at 167°C. This indicates that both the crystalline material as received and the FAM in the final electrospun fibers are mixtures of polymorphs A and B.

XRD powder patterns were used to determine polymorphism of the APIs following electrospinning. Figures 8 and 9 compare the experimental powder patterns to the calculated powder patterns from the Cambridge Structural Database.

For ABZ, both the crystalline material as received and the 1:2 ABZ:PVP electrospun powder patterns show the same peaks as the calculated powder pattern for form I (38) (Fig. 8). The powder patterns for the crystalline ABZ as-received and 1:2 ABZ:PVP electrospun are also consistent with the experimental powder patterns of the commercial form (form I) as presented by Pranzo *et al.* (36). The polymorphism of the ABZ was not affected by the electrospinning process.

The powder patterns for the crystalline FAM as received and 1:2 FAM:PVP electrospun are mixtures of polymorphs A and B (Fig. 9), as can be seen by comparing them to the calculated powder patterns from the Cambridge Structural Database for polymorphs A (39) and B (40). Though many peaks are overlapping, the presence of peaks at both 10.7° 2-theta and 11.7° 2-theta confirm the presence of both polymorphs. Differences in relative peak intensities can be attributed to the difference in sample preparation. The powder samples were flattened onto the zero background plate in a disordered manner, while the electrospun mat was laid onto the plate with all the fibers parallel to the flat plate.

Loading of API in Fibers

The weight percent API in the electrospun fibers was determined using UV-vis spectroscopy. The average loading of ABZ in the fibers was 31 wt% and the average loading of FAM in the fibers was 26 wt%. Compared to the nominal API loading of 33 wt%, both cases showed lower loading than expected, and the reason for this will be addressed in the Discussion section.

Dissolution

Tablets prepared from a powder mixture and electrospun material were subjected to USP dissolution tests to compare the release behavior of API for the two preparation methods. All tablets tested had the same mass and were prepared using the same insertion depth, meaning that the surface area and volume

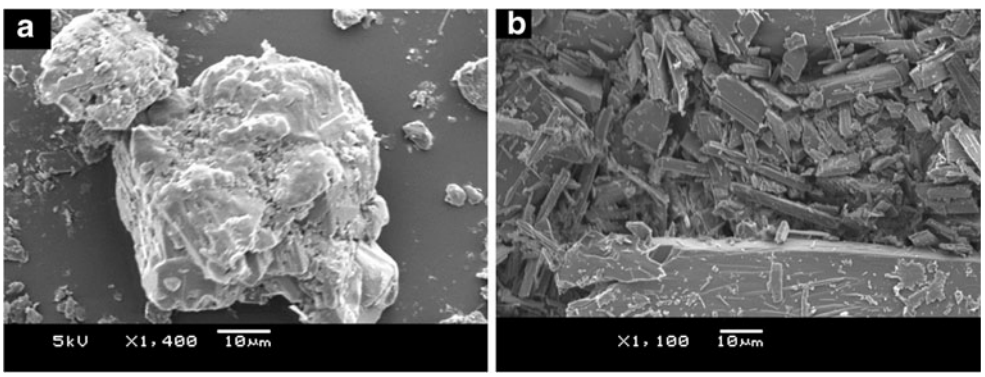

Fig. 4 (**a**) ABZ crystals as received, (**b**) FAM crystals as received.

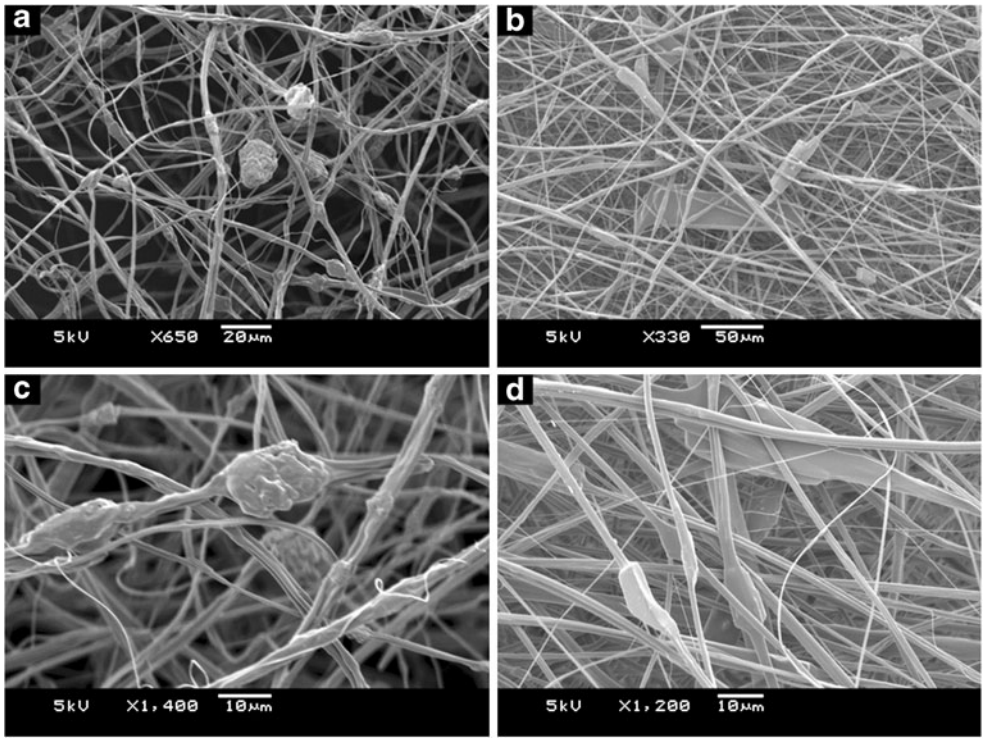

Fig. 5 (**a**) 1:2 ABZ:PVP electrospun fibers, (**b**) 1:2 FAM:PVP electrospun fibers, (**c**) 1:2 ABZ:PVP electrospun fibers at higher magnification, (**d**) 1:2 FAM:PVP electrospun fibers at higher magnification.

of the tablets is the same for all tested. The dissolution curves for ABZ are shown in Fig. 10 and for FAM are shown in Fig. 11, with error bars indicating the standard deviation of the 3 averaged data points.

For both ABZ and FAM, the electrospun formulations showed marked improvement in the dissolution rate over the compressed powder tablets.

DISCUSSION

In order for electrospinning of crystalline API to be usable for pharmaceutical manufacturing, it must be able to be scaled up and the resulting fibers must be well-understood in terms of particle size, extent of dispersion, polymorphism and dissolution properties. In this study, we addressed the former by utilizing free-surface electrospinning to produce suspensions of API in a polymer solution and to address the latter, we characterized the fiber morphology, crystalline properties and dissolution behavior of the final solid dispersion.

Electrospinning API Crystals

We found that the suspensions were spinnable and resulted in fibers with diameters of approximately 1-3 µm. However, for the 1:2 FAM:PVP formulation in particular, the resulting API loading was slightly lower than 33 wt%.

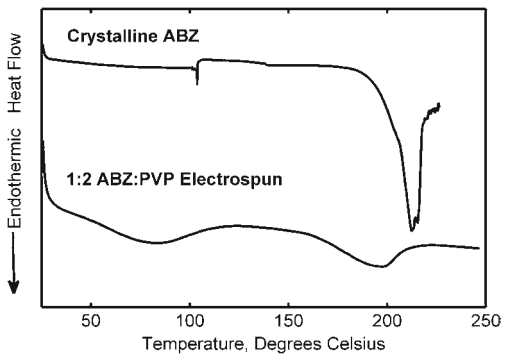

Fig. 6 DSC scans of crystalline ABZ as received and 1:2 ABZ:PVP electrospun.

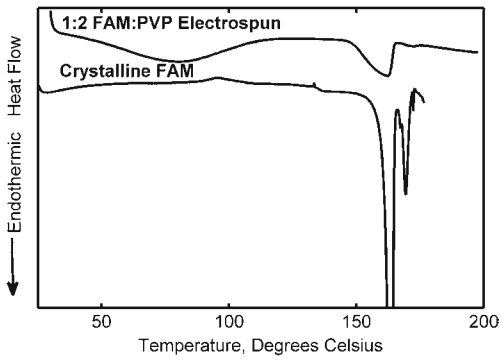

Fig. 7 DSC scans of crystalline FAM as received and 1:2 FAM:PVP electrospun.

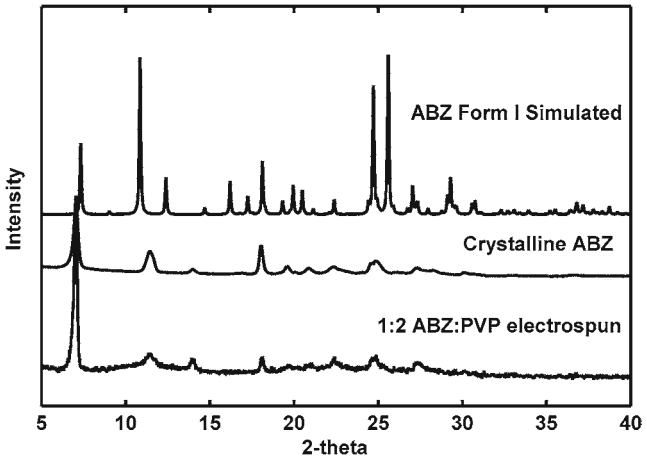

Fig. 8 A calculated XRD powder pattern of ABZ form I (38) and experimental XRD powder patterns of crystalline ABZ as received and 1:2 ABZ:PVP electrospun.

In order to examine why the loading is lower than expected, we calculated the settling velocity, v_s as a function of the particle radius using equation 1:

$$v_s = \frac{2}{9}\frac{\left(\rho_p - \rho_f\right)}{\mu} g R^2 \quad (1)$$

where ρ_f is the fluid density, ρ_p is the particle density, μ is the viscosity, g is the gravitational acceleration and R is the particle radius. The fluid density and viscosity used were the same as 8.6 wt% 1.3 MDa PVP in ethanol used in a previous study (32). The particle densities were taken from the Cambridge Structural Database and were 1.56 g/cm (3) and 1.38 g/cm (3) for FAM (39,40) and ABZ (39), respectively. This velocity is based on Stoke's law and thus is for spherical particles. Though our particles are more plate-shaped, we use a spherical approximation here for simplicity.

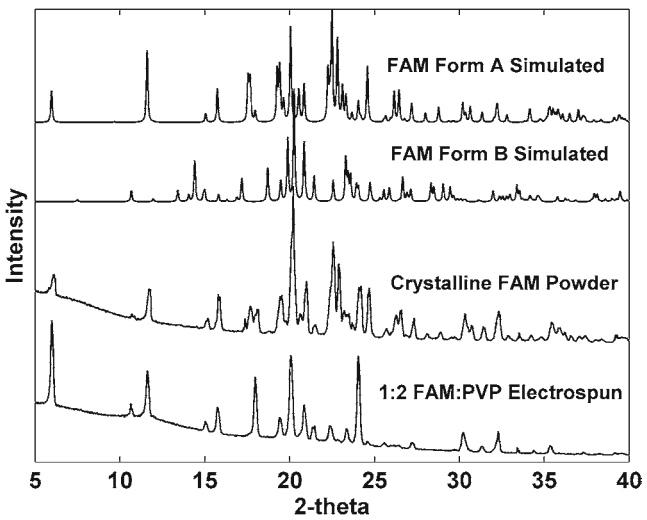

Fig. 9 Calculated XRD powder patterns of FAM forms A (39) and B (41) and experimental XRD powder patterns of crystalline FAM as received and 1:2 FAM:PVP electrospun.

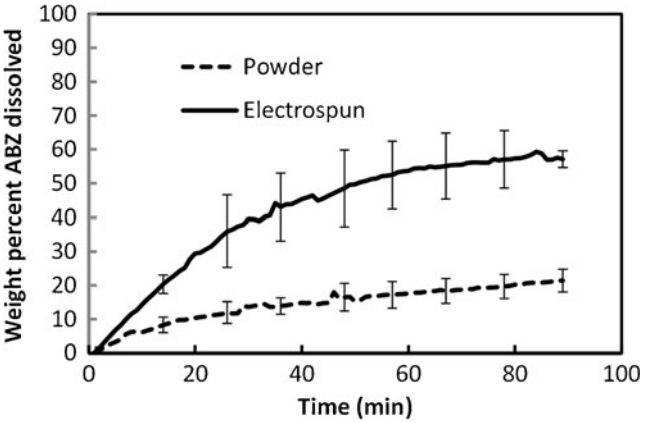

Fig. 10 Dissolution curves for 1:2 ABZ:PVP compressed powder tablets (*dashed line*) and compressed electrospun tablets (*solid line*).

From the settling velocity, we determined the time required for a particle of a given radius to settle to the bottom of the electrospinning bath. The distance between the top of the fluid level when full and the lowest point of the wire rotation is 0.8 cm. Since the particles are dispersed evenly within the fluid at the start of the experiment, we assumed that an average particle must travel 0.4 cm, or half the depth of the bath.

Once the time required to settle is determined for a range of particle diameters, we determined the smallest particle diameter that we expect to settle out in 1 h, the length of our experiment. For ABZ that is 82.5 μm and for FAM that is 70.8 μm. The particle size distribution based on volume percent is known for these solutions from the Malvern results discussed previously, and we have determined that 0.1 vol% ABZ and 4.5 vol% FAM (0.14 wt% ABZ and 7.1 wt% FAM) is expected to settle out during the experiment time, which are of similar magnitude to the difference between the nominal and experimental API loading. These

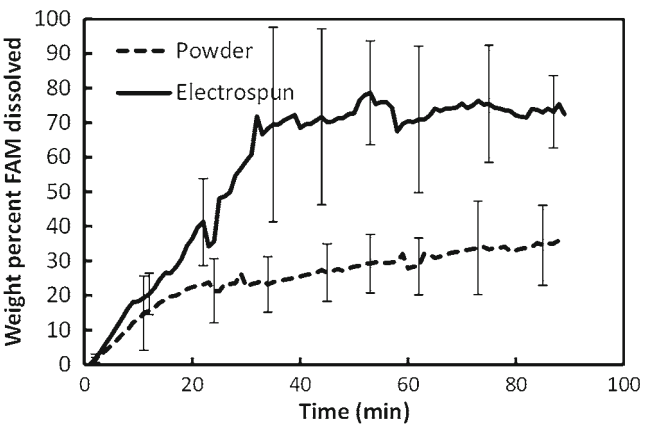

Fig. 11 Dissolution curves for 1:2 ABZ:PVP compressed powder tablets (*dashed line*) and compressed electrospun tablets (*solid line*).

values are merely an estimate, due to the assumptions of spherical particles and the average distance traveled, but they provide insight into the difference in the final API loading in the fibers for the two APIs chosen for this study. For this method to be applied to a large continuous process, a stirring mechanism in the bath or a surfactant must be used to keep the particles suspended.

Characterization of Electrospun Solid Dispersions

The crystal size, the extent of dispersion in the polymer and the crystalline morphology are essential properties of the electrospun API/polymer mixture that will have an effect on the dissolution of the APIs, and thus on the effectiveness of the final formulation. Understanding these properties is essential to the application of this process in a pharmaceutical manufacturing line.

From both the particle size analysis of the spinning suspension and the SEM images, we have determined that the crystals in the electrospun fibers range in size from 0.1–100 μm, with a volume percent-based mean of approximately 10 μm. The crystal size distribution in the compressed powder tablets is the same as that for the suspension prior to sonication, and thus the crystals are larger than those in the electrospun fibers. For ABZ in particular, sonication treatment prior to electrospinning decreased the measured particle size by breaking up aggregates. The crystals are relatively small, and thus are expected to enhance the dissolution rate through an increase in the surface area, as predicted by the Noyes-Whitney equation:

$$\frac{dm}{dt} = \frac{DA}{h}(C_{sat} - C) \tag{2}$$

where $\frac{dm}{dt}$ is the dissolution rate, D is the diffusion coefficient, A is the surface area for diffusion, h is the diffusional path length, C_{sat} is the solubility and C is the concentration in solution (41).

In order to take advantage of the small crystal size to enhance the dissolution rate, the particles must be kept from aggregating. Using electrospinning, this is done by trapping the particles within the small polymer fibers. The SEM images in Fig. 5 show that the particles are present and separated in the polymer fibers. This occurs due to the rapid solvent evaporation following the dispersion using sonication. Once in the dried solid form, the particles remain dispersed until the polymer begins to dissolve during dissolution testing.

Further evidence that the APIs are well-dispersed within the fibers comes from the DSC results. Though the Tg of the polymer can give insight into the mixing level of a polymer and additive, the Tg signal for the polymer was too weak in this case to be measured for the mixtures. Instead, we examine the melting endotherms of the APIs. The depression of the melting points of the APIs and the broadening of the melting endotherms indicate that the APIs are well-dispersed within the fibers and form a partially miscible blend with the polymer as the APIs melt during the temperature ramp of the DSC experiment (42).

As predicted by the Noyes-Whitney equation and supported by the evidence of formation of a well-dispersed solid mixture, the dissolution rate of the API from compressed electrospun tablets is significantly higher than that of the API from compressed powder tablets. As the highly soluble polymer in the electrospun fibers dissolves, the API crystals are released as individual crystals and the exposed surface area is larger than that for agglomerates of API in the compressed powder tablets, resulting in an increased dissolution rate.

CONCLUSIONS

Nanofibers containing a well-mixed dispersion of crystalline API and a polymer were prepared by electrospinning a suspension of crystals in a polymer solution using a high-throughput free surface electrospinning process. The final loading in the fibers was 31 wt% and 26 wt% for 1:2 ABZ:PVP and 1:2 FAM:PVP, respectively, and the APIs retained their crystalline morphology throughout the electrospinning process. Due to the small particle size and dispersion of the particles in the polymer, the dissolution rate was enhanced for compressed electrospun tablets when compared to compressed powder tablets. This study proposes a novel process for preparing solid dispersions of crystalline API *via* electrospinning and demonstrates that the APIs are well-dispersed, retain their polymorphism, and have a high dissolution rate compared to compressed powder tablets. With the advantage that the process may be operated continuously and is powder free, we see that electrospinning would be a viable option for a downstream pharmaceutical manufacturing process.

ACKNOWLEDGMENTS AND DISCLOSURES

We would like to acknowledge Novartis AG for funding and support of this work. We would also like to thank Keith M. Forward for aid with free-surface electrospinning and Keith Chadwick for his input on XRD interpretation.

REFERENCES

1. Plumb K. Continuous processing in the pharmaceutical industry: Changing the mind set. Chem Eng Res Des. 2005;83(6):730–8.
2. Breitenbach J. Melt extrusion: from process to drug delivery technology. Eur J Pharm Biopharm. 2002;54(2):107–17.

3. Bell ER, Massachusetts Institute of Technology. Melt extrusion and continuous manufacturing of pharmaceutical materials [PhD Thesis]. Cambridge, MA: Massachusetts Institute of Technology; 2011.
4. Kim W, Massachusetts Institute of Technology. Layer bonding of solvent-cast thin films for pharmaceutical solid dosage forms [Master's Thesis]. Cambridge, MA: Massachusetts Institute of Technology; 2010.
5. Brettmann BK, Bell E, Myerson AS. and Trout B L, Solid-state NMR characterization of high-loading solid solutions of API and excipients formed by electrospinning. J Pharm Sci. 2012;101(4):1538–45.
6. Buschle-Diller G, Cooper J, Xie Z, Wu Y, Waldrup J. Release of antibiotics from electrospun bicomponent fibers. Cellulose. 2007;14:553–62.
7. Yu D, Zhang X, Shen X. Brandford–White C, Zhu L. Ultrafine ibuprofen–loaded polyvinylpyrrolidone fiber mats using electrospinning. Polym Int. 2009;58:1010–3.
8. Verreck G, Chun I, Peeters J, Rosenblatt J, Brewster ME. Preparation and characterization of nanofibers containing amorphous drug dispersions generated by electrostatic spinning. Pharm Res. 2003;20:810–7.
9. Verreck G, Chun I, Rossenblatt J, Peeters J, Van Dijck A, Mensch J, Noppe M, Brewster ME. Incorporation of drugs in an amorphous state into electrospun nanofibers composed of a water-insoluble, nonbiodegradable polymer. J Control Release. 2003;92:349–60.
10. Ramakrishna S. An Introduction to Electrospinning and Nanofibers. Singapore: World Scientific Publishing Company; 2005.
11. Lukas D, Sarkar A, Pokorny P. Self-organization of jets in electrospinning from free liquid surface: a generalized approach. J Appl Phys. 2008;103(8):084309.
12. Yarin AL, Zussman E. Upward needleless electrospinning of multiple nanofibers. Polymer. 2004;45(9):2977–80.
13. Miloh T, Spivak B, Yarin AL. Needleless electrospinning: electrically driven instability and multiple jetting from the free liquid surface of a spherical liquid layer. J Appl Phys. 2009;106(11):114910.
14. Kostakova E, Meszaros L, Gregr J. Composite nanofibers produced by modified needleless electrospinning. Mater Lett. 2009;63 (28):2419–22.
15. Jirsak O, Sysel P, Sanetrnik F, Hruza J, Chaloupek J. Polyamic acid nanofibers produced by needleless electrospinning. J Nanomater. 2010 Jan; ID842831.
16. Niu H, Lin T, Wang X. Needleless electrospinning. I. a comparison of cylinder and disk nozzles. J Appl Polym Sci. 2009;114 (6):3524–30.
17. Wang X, Niu H, Lin T. Needleless electrospinning of nanofibers with a conical wire coil. Polym Engr Sci. 2009;49(8):1582–6.
18. Lu B, Wang Y, Liu Y, Duan H, Zhou J, Zhang Z, Wang Y, Li X, Wang W, Lan E. Superhigh-throughput needleless electrospinning using a rotary cone as spinneret. Small. 2010;6(15):1612–6.
19. Varabhas JS, Tripatanasuwan S, Chase GG, Reneker DH. Electrospun jets launched from polymeric bubbles. J Eng Fibers Fabr. 2009;4:46–50.
20. Forward KM, Rutledge GC. Free surface electrospinning from a wire electrode. Chem Eng J. 2012;183:492–503.
21. Tungprapa S, Jangchud I, Supaphol P. Release characteristics of four model drugs from drug-loaded electrospun cellulose acetate fiber mats. Polymer. 2007;48(17):5030–41.
22. Yu DG, Shen XX, Branford-White C, White K, Zhu LM, Bligh SWA. Oral fast-dissolving drug delivery membranes prepared from electrospun polyvinylpyrrolidone ultrafine fibers. Nanotechnology. 2009;20(5):055104.
23. Hancock BC, Zografi G. Characteristics and significance of the amorphous state in pharmaceutical systems. J Pharm Sci. 1997;86 (1):1–12.
24. Chew SY, Hufnagel TC, Lim CT, Leong KW. Mechanical properties of single electrospun drug-encapsulated nanofibres. Nanotechnology. 2006;17(15):3880–91.
25. Natu MV, de Sousa HC, Gil MH. Effects of drug solubility, state and loading on controlled release in bicomponent electrospun fibers. Int J Pharm. 2010;397(1–2):50–8.
26. Ignatious F, Sun L, Lee C-P, Baldoni J. Electrospun nanofibers in oral drug delivery. Pharm Res. 2010;27(4):576–88.
27. Wang M, Singh H, Hatton TA, Rutledge GC. Field-responsive superparamagnetic composite nanofibers by electrospinning. Polymer. 2004;45(16):5505–14.
28. Tiwari MK, Yarin AL, Megaridis CM. Electrospun fibrous nanocomposites as permeable, flexible strain sensors. J Appl Phys. 2008;103(4):044305.
29. Salalha W, Kuhn J, Dror Y, Zussman E. Encapsulation of bacteria and viruses in electrospun nanofibers. Nanotechnology. 2006;17 (18):4675–81.
30. Wang M, Hsieh AJ, Rutledge GC. Electrospinning of poly(MMA-co-MAA) copolymers and their layered silicate nanocomposites for improved thermal properties. Polymer. 2005;46(10):3407–18.
31. Wang M, Yu JH, Hsieh AJ, Rutledge GC. Effect of tethering chemistry of cationic surfactants on clay exfoliation, electrospinning and diameter of PMMA/clay nanocomposite fibers. Polymer. 2010;51(26):6295–302.
32. Brettmann B, Tsang S, Forward K, Rutledge G, Myerson AS, Trout BL. Free Surface Electrospinning of Microparticles. Langmuir. 2012;28(25):9714–21.
33. Lim J-M, Moon JH, Yi G-R, Heo C-J, Yang S-M. Fabrication of one-dimensional colloidal assemblies from electrospun nanofibers. Langmuir. 2006;22(8):3445–9.
34. U.S. Pharmacopeia Reference Tables. USP29-NF24. www.pharmacopeia.cn. Accessed Aug 5, 2012.
35. Dror Y, Salalha W, Khalfin RL, Cohen Y, Yarin AL, Zussman E. Carbon nanotubes embedded in oriented polymer nanofibers by electrospinning. Langmuir. 2003;19(17):7012–20.
36. Pranzo MB, Cruickshank D, Coruzzi M, Caira MR, Bettini R. Enantiotropically related albendazole polymorphs. J Pharm Sci. 2010;99(9):3731–41.
37. Lu J, Wang X-J, Yang X, Ching C-B. Polymorphism and Crystallization of Famotidine. Cryst Growth Des. 2007;7(9):1590–8.
38. Cambridge Structural Database, reference code BOGFUZ
39. Cambridge Structural Database, reference code FOGVIG06
40. Cambridge Structural Database, reference code FOGVIG07
41. Leuner C, Dressman J. Improving drug solubility for oral delivery using solid dispersions. Eur J Pharm Biopharm. 2000;50:47–60.
42. Marsac PJ, Li T, Taylor LS. Estimation of drug–polymer miscibility and solubility in amorphous solid dispersions using experimentally determined interaction parameters. Pharm Res. 2008;26 (1):139–51.